12/4/2007 9:59 AM

Synthesis and Evaluation of [*N-methyl*-^{11}C]*N*-Desmethyl-loperamide as a New and Improved PET Radiotracer for Imaging P-gp Function

Neva Lazarova, Sami S. Zoghbi, Jinsoo Hong, Nicholas Seneca, Edward Tuan, Robert Gladding, Jeih-San Liow, Andrew Taku, Robert B. Innis and Victor W. Pike*

Molecular Imaging Branch, National Institute of Mental Health, National Institutes of Health, Bethesda, Maryland 20892, USA.

*Author for correspondence: Dr. V. W. Pike, Molecular Imaging Branch, National Institute of Mental Health, National Institutes of Health, Building 10, Room B3 C346A, 10 Center Drive, Bethesda, MD 20892-1103, USA. Tel. 301 594 5986. FAX 301 480 5112. e-mail: pikev@mail.nih.gov.

Word count: (current 7,003)

Running header: Synthesis and Assessment of [^{11}C]*N*-Desmethyl-loperamide

Abbreviations: DAT, dopamine transporter; DCPQ, ((*2R*)-*anti*-5-{3-[4-(10,11-dichlromethanodibenzosuber-5-yl)piperazin-1-yl]-2-hydroxypropoxy}quinoline trihydrochloride; DIPEA, *N*,*N*-di-isopropylethylamine; dLop, *N*-desmethyl-

loperamide;.NET, noradrenaline transporter; PET, positron emission tomography; P-gp, P-glycoprotein; SPECT, single photon emission computed tomography;

Abstract (150 words max; current 148)

[^{11}C]Loperamide has been proposed for imaging P-glycoprotein (P-gp) function with positron emission tomography (PET), but its metabolism to [*N-methyl*-^{11}C]*N-desmethyl*-loperamide ([^{11}C]dLop; [^{11}C]**3**) precludes quantification. We considered that [^{11}C]**3** might itself be a superior radiotracer for imaging brain P-gp function, and therefore aimed to prepare [^{11}C]**3** and characterize its efficacy. An amide precursor (**2**) was synthesized and methylated with [^{11}C]iodomethane to give [^{11}C]**3**. After administration of [^{11}C]**3** to wild type mice, brain radioactivity uptake was very low. In P-gp (*mdr-1a*(−/−)) knockout mice, brain uptake of radioactivity increased about 3.6 fold (by PET measures), and over 7 fold (by ex vivo measures). In knockout mice, brain radioactivity was predominantly (90%) unchanged radiotracer. In monkey PET experiments, brain radioactivity uptake was also very low, and after P-gp blockade increased about five-fold. [^{11}C]**3** is an effective new radiotracer for imaging brain P-gp function and, in favor of future successful quantification, appears free of extensive brain-penetrant radiometabolites.

Keywords: P-gp; PET; radiotracer; carbon-11, *N*-desmethyl-loperamide

Introduction

P-Glycoprotein (P-gp) is a protein that functions as an ATP-dependent efflux pump for a wide range of xenobiotics at the blood-brain barrier[1] and at membrane barriers in several other organs[2], such as small intestine, liver and kidney. P-gp is also often highly expressed in tumors.[2] Hence P-gp can be a severe obstacle to the penetration of established or developmental drugs into the targeted organ or tumor.[3] In neurology, P-gp may, for example, be an obstacle to the brain penetration of anti-HIV drugs.[4] In oncology, P-gp plays a major role in 'multi-drug resistance'[5], which is directly responsible for the failure of a high proportion of attempted chemotherapy. Altered expression of P-gp may also contribute to the progression of neurodegenerative disorders, such as Alzheimer's disease[6,7,8], HIV encephalitis[9] and Parkinson's disease[10]. Hence, elucidating the expression and function of P-gp in human subjects in vivo could be of great importance in both drug development and medicine. Moreover, in the field of developing molecular imaging agents for use with positron emission tomography (PET) or single photon emission computed tomography (SPECT), the effect of P-gp is also frequently encountered, for example, in limiting the brain entry of some neuroreceptor radioligands[11,12]. These same imaging modalities, with radiotracers based on P-gp substrates, have been proposed for

examining P-gp function in vivo (for a review, see reference13). The most widely examined radiotracers include [^{11}C]colchicine[14] , [^{11}C]verapamil[15,16] , [^{11}C]daunorubicin[15], [^{18}F]paclitaxel [17] , [^{94m}Tc]sestamibi [18] and [^{11}C]loperamide[19,20] for PET, and [^{99m}Tc]sestamibi for SPECT[21]. Many of these radiotracers suffer from one or more limitations (e.g. difficult radiosynthesis, low sensitivity or troublesome metabolism), which have so far compromised their use for sensitive and quantitative assessment of P-gp function in vivo, especially in human subjects.

Loperamide is sold over-the-counter as an antidiarrheal agent (Imodium™) which acts through agonism of gut μ-opioid receptors.[22] This drug is normally without harmful central effects solely because P-gp excludes it from brain.[23] We were attracted to [^{11}C]loperamide (**Figure 1**) as a prospective radiotracer for evaluating brain P-gp function in brain, because of its safety in human subjects and apparent ease of radiosynthesis[15,16]. However, our initial investigations [24] , showed that [^{11}C]loperamide is heavily metabolized. Demethylation [25 , 26] of [^{11}C]loperamide gave [*N-methyl*-^{11}C]*N*-desmethyl-loperamide ([^{11}C]dLop; [^{11}C]**3**; **Figure 1**) as a radiometabolite that also behaved as an avid substrate for P-gp.24 The penetration of [^{11}C]**3** into brain, under conditions in which P-gp is absent or inhibited, thwarts any possibility of quantitative analysis of P-gp function with [^{11}C]loperamide and PET. We

considered that [^{11}C]**3** itself could be a superior radiotracer, mainly because its metabolism might be expected to be less troublesome for eventual quantification of brain P-gp function. Thus, metabolism of [^{11}C]**3** is also expected to occur by demethylation[26], but to lead only to single carbon radiometabolites, such as [^{11}C]methanol. Such radiometabolites will ultimately be oxidized and expired as [^{11}C]carbon dioxide; they should not accumulate in tissues accessed by the radiotracer to cause difficulty in biomathematical analysis of acquired PET data. Moreover, as a known metabolite of loperamide, **3** would be safe to administer to human subjects in tracer doses. This study describes an effective synthesis of [^{11}C]**3** for its safe intravenous administration (**Scheme 1**) and the evaluation of [^{11}C]**3** in mice and monkey with PET. [^{11}C]**3** shows highly favorable properties as a new radiotracer for the potential quantification of brain P-gp function.

Results

Chemistry. Compound **1** was obtained in 69% yield by alkylation of 4-(4-chlorophenyl)-4-hydroxylpiperidine with 4-bromo-2,2-diphenylbutyronitrile in the presence of DIPEA (**Scheme 1**). Slow hydrolysis of **1** with KOH in ^{t}BuOH gave the required precursor **2** in 37% yield. Methylation of **2** with iodomethane gave **3** in low yield, but in adequate amount to serve as a chromatographic reference material.

[^{11}C]**3** was prepared, ready for intravenous injection, from **2** in 18 ± 2% (*n* = 20) isolated decay-corrected radiochemical yield from cyclotron-produced [^{11}C]carbon dioxide. The radiosynthesis required 40 min. The obtained activity of [^{11}C]**3** averaged 1.9 ± 0.8 GBq. Specific radioactivity, decay-corrected to the end of synthesis, averaged 152 ± 48 GBq/μmol. Radiochemical purity exceeded 99% and the product was radiochemically stable for at least 1 h (by radio-HPLC analysis). [^{11}C]**3** was well separated with HPLC from precursor **2** and other impurities (**Figure 2**). Thus, chemical impurities were low (estimated as < 1 nmol per batch, by assuming that the impurities have the same extinction coefficient in the radio-HPLC analysis with an absorbance detector set to 225 nm).

Computation of *cLogP* and *cLogD,* and Measurement of *LogD*. *cLogP* and *cLogD* (at *pH* = 7.4) values for **3** were 4.16 and 3.49, respectively. The measured *LogD* value of [^{11}C]**3** was much lower 2.60 ± 0.04 (*n* = 6).

Pharmacological Screen of 3. At 10 μM concentration, **3** was found to cause < 50% inhibition of binding to 5-HT$_{1A,1B,1D,1E,2A,2B}$, $\beta_{1,2}$, $D_{1,2,5}$, $M_{1\text{-}5}$, κ- and δ-opiate receptors, and to NET and DAT. Greater than 50% inhibition was observed at $\alpha_{1A,2A\text{-}C}$, $D_{3,4}$, $H_{1,3}$, μ–opiate and $\sigma_{1,2}$ receptors and SERT.

Corresponding K_i values (nM) were α_{1A} (9.9), α_{2A} (0.98), α_{2B} (7.01), α_{2C} (2.4), H_1 (4.2), H_3 (9.3) and μ–opiate (0.56), and SERT (6.2) .

PET Imaging of [^{11}C]3 in Mouse Brain. After the injection of the [^{11}C]**3** into wild type mice, the brain uptake of radioactivity measured with PET reached a very low maximum between 2 and 4 min. In P-gp knockout mice, maximal brain uptake of radioactivity was higher and occurred between 8 and 20 min. The subsequent washout of brain radioactivity from all mice was slow. At 35 min after radiotracer injection forebrain and cerebellar uptakes of radioactivity were on average 2.5 and 1.87 fold higher in the knockout than in the wild type mice, respectively (**Figure 3**).

Measurement of [^{11}C]3 and Radiometabolites in Mouse Plasma and Brain. Recoveries of radioactivity from brain tissue and plasma into acetonitrile were between 87.0 and 97.1% (92.5 ± 2.9%, n = 18). Radioactive analytes were fully recovered from the HPLC column.

At 30 min after the administration of [^{11}C]**3**, the radioactivity concentrations found in plasma were low and very similar between knockout and wild type mice (**Table 1**). By contrast, radioactivity concentrations in the forebrains and cerebella of knockout mice were more than 7- and 8-fold higher,

respectively, than the very low concentrations found in wild type mice (**Table 1**).

Three radiometabolites ([^{11}C]A−[^{11}C]C), all less lipophilic than [^{11}C]**3**, were detected in mice plasma and brain tissue samples at 30 min after radiotracer injection (**Figure 4**). The concentrations of unchanged [^{11}C]**3** in plasma were on average very low and similar between wild type mice (2.8% SUV) and knockout (1.7% SUV) (**Table 1**).

On average, [^{11}C]**3** was 43.6% and 45.5% of radioactivity in forebrains and cerebella of wild type mice, while in the knockout mice these values increased to 91.3% and 88.9%, respectively. The uptake of [^{11}C]**3** was over 15-fold higher in cerebellum and forebrain of knockout mice than in wild type mice (**Table 1**).

In knockout mice, [^{11}C]C was the most prevalent radiometabolite in brain, despite its very low presence in plasma (**Table 1**). Although this radiometabolite was over ten-fold higher in concentration in forebrain and cerebellum of P-gp knockout mouse than in wild type mice, the absolute concentrations in knockout mice were very low compared to that of [^{11}C]**3**. The more polar radiometabolites, [^{11}C]A and [^{11}C]B, showed no significant increase in brain uptake in knockout mice compared to wild type mice (**Table 1**).

Finally, the ratios of [^{11}C]**3** concentration in forebrain and cerebellum to that in plasma were close to unity for wild type mice but increased to over twenty for knockout mice (**Table 1**).

PET Imaging of Monkey Brain with [^{11}C]3. After intravenous injection of [^{11}C]**3** into monkey under baseline conditions, uptake of radioactivity into brain regions was maximally very low but well retained (**Figure 5A**). Frontal cortex showed highest uptake and cerebellum lowest (data for other cortical regions were intermediate and are not shown). In the P-gp pre-block experiment, radioactivity was taken up more avidly in all measured brain regions, reaching maxima within 30 min (**Figure 5B**). There was some regional variation in brain uptake with putamen showing highest uptake and frontal cortex showing lowest. In this experiment, the ratio of maximal brain radioactivity to that in the baseline experiment was about five.

In both baseline and P-gp blocked experiments there was a very high and similar uptake of radioactivity outside the blood-brain barrier in the pituitary (**Figure 5**).

PET images of monkey brain obtained by summing data acquired between 20 and 90 min after intravenous injection of [^{11}C]**3** under baseline conditions confirmed uniformly very low uptake of radioactivity into brain (**Figure 6A**), but high uptake into pituitary. By contrast, radioactivity was

taken up into all brain in the corresponding pre-block experiment, and also seen again in pituitary (**Figure 6B**).

In the PET experiment in which P-gp was inhibited with DCPQ, and also the opiate receptor antagonist, naloxone, was administered at 30 min after injection of [^{11}C]**3**, there was again high early uptake of radioactivity into all examined brain regions. By visual inspection, naloxone had no effect on the rate of washout of radioactivity from these brain regions (c.f. **Figure 7** with **Figure 5B**). The uptake of radioactivity into pituitary was unaffected by administration of DCPQ at either 8 mg/kg or 16 mg/kg i.v. before injection of [^{11}C]**3** (**Figure 8**). Moreover, the administration of naloxone at 30 min after radiotracer injection again had no effect on washout of radioactivity from pituitary compared to the rate of washout in the baseline experiment (**Figure 8**).

Emergence of Radiometabolites of [^{11}C]3 in Monkey Plasma. After intravenous injection of [^{11}C]**3** into monkey under baseline or P-gp blocked conditions, radioactivity was cleared rapidly and at very similar rates from whole blood (**Figure 9**). The recovery of radioactivity from plasma into acetonitrile supernatants for radio-HPLC analysis was highly efficient with only very low percentages of radioactivity co-precipitated with protein. [^{11}C]**3** and three less polar radiometabolites were detected in plasma. The clearance of unchanged [^{11}C]**3** from monkey plasma was rapid and unaffected by pre-

administration of DCPQ (**Figure 10**). The radiometabolites had similar retention times to those observed in mouse plasma and brain. Radiometabolite B only ever became a low percentage of radioactivity in plasma, but radiometabolites A and C gradually increased as a percentage of total radioactivity (**Figure 11**). In the baseline and P-gp blocked experiments, the times taken for radiometabolite activity to equal that of [^{11}C]**3** were very similar (~ 45 min). DCPQ had little effect on the rate at which each radiometabolite emerged in plasma.

Discussion

In order to prepare [^{11}C]**3,** it was necessary to devise a convenient synthesis of the primary amide **1,** a compound which, as far as we are aware, has only been mentioned once in the literature, but without synthesis details.[27] The synthesis of **1** was accomplished in two steps from commercially available materials. Slow hydrolysis of **1** to **2** with potassium hydroxide in ^{t}butanol proved to be a key step; attempts to achieve this step with a multitude of other reagents were unsuccessful. A small quantity of reference **3** was obtained by alkylation of **2** with iodomethane.

[^{11}C]**3** was readily prepared for intravenous injection by alkylation of **2** with [^{11}C]iodomethane, itself prepared from cyclotron-produced [^{11}C]carbon dioxide. The whole radiosynthesis was performed in a lead-shielded hot-cell

with automated apparatus. Purification by reverse phase HPLC gave [^{11}C]**3** in high radiochemical and chemical purity, and high specific radioactivity. The level of specific radioactivity is unlikely to be critical for this radiotracer since it is not targeted at imaging a saturable binding site. The formulated radiotracer was radiochemically stable.

The measured *LogD* value of [^{11}C]**3** was found to be 2.60 and appreciably different to the computed value (3.49). The measured value lies in the range normally considered favorable for good penetration of the blood-brain barrier (in the absence of any effect of efflux transporters).[28,29]

Loperamide has high affinity for μ-opiate receptors.[30] A pharmacological screen found that **3** has high affinity for μ-opiate receptors (K_i = 0.56 nM), and also quite high affinity (K_i = < 10 nM) for $\alpha_{1A,,2A-2C}$, $D_{3,4}$, $H_{1,3}$, and $\sigma_{1,2}$ receptors and SERT, but was devoid of high affinity for any of a wide battery of other receptors, transporters and binding sites. This pharmacological profile is similar to that of loperamide itself.

PET scans of wild type mice administered [^{11}C]**3** alone revealed only very low uptake of radioactivity into brain which quickly maximized (**Figure 2A**). Radioactivity uptake was similar in forebrain and cerebellum and in each case was followed by slow washout of radioactivity. These data are consistent with effective exclusion of the radiotracer from brain by P-gp at the blood-brain

barrier. In P-gp knockout mice, the uptake of radioactivity was two– to three fold higher in forebrain and cerebellum than in the wild type mice (**Figure 2B**). These results provide direct evidence that [^{11}C]**3** is a substrate for P-gp, in accord with prediction from our earlier study**Error! Bookmark not defined.**.

PET scans are unable to identify the chemical species being measured in brain. Moreover, they are subject to partial volume effects due to the limited spatial resolution of the PET camera. In these experiments the spatial resolution was ~ 1.8 mm fwhm and therefore quite comparable to small structures in mouse brain (~ 0.4 g; ~ 0.75 cm^3). Small regions of mouse brain containing relatively high levels of radioactivity would not therefore be measured accurately. They would be underestimated while any neighboring regions of low activity would be overestimated. In order to measure radioactivity concentration in brain more accurately and to identify the chemical identity of the radioactivity, experiments were performed to allow ex vivo measurement of radioactivity in brain at a single time point with a γ-counter. Corresponding measurements were also made in plasma. The time chosen for these measurements was 30 min after [^{11}C]**3** injection, since the PET scans had already shown that there was little loss of activity from brain over the preceding time span (**Figure 3**). Radio-HPLC of brain tissue (**Figure 4**) or plasma was used to identify unchanged radiotracer and its radiometabolites.

Radio-HPLC of wild type or P-gp knockout plasma showed that a high proportion of radioactivity consisted of radiometabolites, all of which were less lipophilic than parent radiotracer. Measurements in wild type and knockout mouse gave very similar values for total radioactivity concentration in plasma and for the distribution of this radioactivity between radiotracer and radiometabolites (**Table 1**).

Measurements on brain tissue confirmed the higher radioactivity content in the P-gp knockout mice. The ratios of radioactivities in knockout mouse forebrain and cerebellum to that in wild type mice were 7.2 and 7.9, respectively compared to the values of (~ 3.6−3.7) seen between 27.5 and 35 min in the PET experiments. The PET ratio is therefore in appreciable error.

Blood constitutes 4−5% of brain volume. The PET scans are uncorrected for blood radioactivity while the ex vivo measures do not include significant blood radioactivity. However, in this case blood radioactivity is not a major source of error in the PET measurements because the blood levels of radioactivity are either similar to that in brain (in wild type mice) or twenty-fold lower (in knockout mice) (**Table 1**).

The several-fold higher uptake of radioactivity into forebrain and cerebellum of the knockout mice compared to the wild type is predominantly explained by the greatly increased uptake of [^{11}C]**3**. In the knockout mouse,

uptake of [^{11}C]**3** increases about fifteen-fold in both forebrain and cerebellum. As a result about 90% of the radioactivity in knockout mouse brain is unchanged [^{11}C]**3** (**Table 1**). This result, obtained in a generally highly metabolic species, augers well for the potential to quantify brain P-gp function with PET and [^{11}C]**3** in rodents and higher species, including humans. By contrast, only ~ 50% of the radioactivity in P-gp knockout mouse brain after the administration of [^{11}C]loperamide is unchanged radiotracer, so precluding prospects for quantification of P-gp function.**Error! Bookmark not defined.** Hence, on the basis of these data in mice, [^{11}C]**3** is a vastly better radiotracer than [^{11}C]loperamide.

Encouraged by these results, we pursued PET experiments in monkey in which DCPQ at doses equal to or greater than 8 mg/kg i.v. could be used to block brain P-gp.**Error! Bookmark not defined.** Structurally, DCPQ is very closely related to zosuquidar (LY335979) (**Figure 12**), which shows selectivity for P-gp versus other efflux transporters, such as MRP1, MRP2, MRP3 or BCRP.[31,32]

In a baseline PET experiment with [^{11}C]**3** in monkey, the uptake of radioactivity into all examined brain regions was very fast, low and retained (**Figure 5A**). In striking contrast there was a very high uptake of radioactivity into the pituitary which lies outside the blood-brain barrier. In an experiment in

the same monkey in which DCPQ was administered before [^{11}C]**3**, radioactivity uptake into all brain regions increased dramatically, while the uptake into pituitary was very similar to that in the baseline experiment (**Figure 5B**). PET images of the brain and pituitary under baseline and P-gp blocked conditions dramatically portray these patterns (**Figure 6**). These data are consistent with [^{11}C]**3** behaving as a substrate for P-gp at the blood–brain barrier, but not at the pituitary which lies outside the blood-brain barrier.

The time-activity curves under baseline and P-gp blocked conditions are characterized by fast initial uptake of radioactivity and then strong retention of radioactivity (**Figure 6**). Furthermore, there is regional variation in the uptake of radioactivity. Regional variations in blood flow to brain may be a strong contributor to the initial distribution of radioactivity. A further possibility is that regional variations in radioactivity distribution relate to variations in the distribution of P-gp. These possibilities require future extensive investigation. Quantitative measures of P-gp distribution throughout brain regions are presently unknown.

In view of the high affinity shown by **3** for a variety of receptors and SERT, it was considered that the strong retention of radioactivity in all brain regions might represent tight binding of radiotracer to one or more of these sites. **3** showed highest affinity for μ-opiate receptors. Naloxone is a high

affinity (μ, κ and δ) opiate receptor antagonist that has been successfully to displace PET radioligands, such as [^{11}C]diprenorphine[33,34], [^{11}C]GR103545[35] and [^{11}C]methylnaltrindole[36], from opiate receptors in monkey and human brain. Therefore, we attempted to displace radioactivity in brain with an injection of naloxone at 30 min after the administration of [^{11}C]**3** to P-gp inhibited monkey. There was no discernible change in the rate washout of radioactivity from any of the examined brain regions (**Figure 7**). We conclude that specific binding to opiate receptors was not responsible for the strong retention of radioactivity in brain. Likewise, there was no effect of nalaxone on washout of radioactivity from pituitary in the same experiment (**Figure 8**), even though pituitary is know to contain high levels of opiate receptors. The uptake of radioactivity into pituitary was independent of P-gp inhibition or amount of inhibitor (DCPQ) administered, showing uptake is not affected by P-gp. Most probably the uptake of radioactivity in brain and pituitary represents non-specific binding to high concnetration non-saturable sites.

The retention of radioactivity in brain will depend on the input of radioactive species from the blood. The clearance of radioactivity from blood was initially rapid, reaching a very low stable radioactivity level at 20 min. This clearance was unaffected by pre-administration of DCPQ (**Figure 9**). The clearance of parent radiotracer was also fast initially, but continued slowly after

20 min. This slow clearance of radiotracer from blood may explain the slow clearance of radioactivity from brain. Again the clearance of radiotracer was unaffected by pretreatment with DCPQ (**Figure 10**).

Three radiometabolites were found in monkey blood after administratio n of [^{11}C]**3**. These were all less lipophilic than [^{11}C]**3** and had similar retention times to those seen in mouse plasma. The same radiometabolites may therefore be produced in mouse and monkey. The pattern for the emergence of these radiometabolites in plasma was unaffected by DCPQ pre-treatment (**Figure 11**). The time taken for half the radioactivity in plasma to be represented by radiometabolites was about 45 min (significantly slower than for [^{11}C]loperamide[24]).

Conclusion

[^{11}C]**3** was confirmed to be an avid substrate for brain P-gp in mouse and monkey. Although [^{11}C]**3** was quite rapidly metabolized to three less polar radiometabolites, under conditions in which P-gp is absent or blocked radioactivity uptake into brain was greatly increased. In P-gp knockout mouse the vast majority of radioactivity entering brain was unchanged [^{11}C]**3** in high ratio to its concentration in plasma. These findings show that [^{11}C]**3** is a new radiotracer with favorable properties for quantifying brain P-gp function with PET.

Experimental

Materials and general methods. All reagents and organic solvents were ACS grade or higher and used without further purification. 4-(4-Chlorophenyl)-4-hydroxypiperidine, 4-bromo-2,2-diphenylbutyronitrile and *N*,*N*-di-isopropylethylamine (DIPEA) were purchased from Aldrich (Milwaukee, WI). DCPQ ((2*R*)-*anti*-5-{3-[4-(10,11-dichloromethanodibenzo-suber-5-yl)piperazin-1-yl]-2-hydroxypropoxy}quinoline trihydrochloride[37] was a gift from Eli Lilly (Indianapolis, IN).

Reactions were performed under argon atmosphere with standard Schlenk techniques. Yields are recorded for chromatographically and spectroscopically (^{1}H and ^{13}C NMR) pure materials.

^{1}H (400 MHz) and ^{13}C NMR (100 MHz) spectra of all compounds were recorded on an Avance 400 spectrometer (Bruker; Billerica, MA). Chemical shifts are reported in δ units (ppm) downfield relative to the chemical shift for tetramethylsilane. Abbreviations br, s, d, t and m denote broad, singlet, doublet, triplet and multiplet, respectively.

Mass spectra were obtained on a Polaris-Q GC-MS instrument (Thermo Fisher Scientific Corp., Waltham, MA). LC-MS was performed on a LCQ Deca instrument (Thermo Fisher Scientific Corp.) equipped with a reverse-phase HPLC column (Synergi Fusion-RP, 4 μm, 150 × 2 mm; Phenomenex,

Torrance, CA). The instrument was set up to perform electrospray ionization (spray voltage 5 kV, nitrogen sheath flow 65 units, auxiliary gas flow 10 units, capillary voltage 35 V and capillary temperature 260 °C). For the characterization of synthesized compounds, the column was eluted at 150 μL/min, either isocratically or with a gradient between H_2O: MeOH: AcOH (90: 10: 0.5 by vol.) and MeOH: AcOH (100: 0.5 v/v). High resolution mass spectra (HRMS) were acquired at the Mass Spectrometry Laboratory, University of Illinois at Urbana Champaign (Urbana, IL) under electron ionization conditions with a double-focusing high resolution instrument (Autospec; Micromass Inc.). Samples were introduced through a direct insertion probe.

Thin layer chromatography (TLC) was performed on silica gel layers (type 60 F254; EMD Chemicals, Gibbstown, NJ), and compounds were visualized under UV light and by staining with Dragendorff's reagent (Sigma Aldrich, St Louis, MO).

Melting points were measured with a Mel-Temp manual melting point apparatus (Electrothermal; Fisher Scientific, USA), and were uncorrected.

[^{11}C]**3** and its radiometabolites in samples of biological material were analyzed on a Nova-Pak® C18 column (4 μm, 100 × 8 mm; Waters Corp., Milford, MA) housed within a radial compression module (RCM 100). The

column was eluted with MeOH: H_2O: Et_3N (70: 30: 0.1 by vol.) at 2.0 mL/min, with eluate monitored with a flow through Na(Tl) scintillation detector (Bioscan, Washington, DC). Methanol (2 mL) was injected onto the column to show no residual radioactivity after each analysis run. Chromatographic data were corrected for physical decay to the time of HPLC injection, stored and analyzed by "Bio-Chrom Lite" software (Bioscan). The same HPLC method was applied for the determination of radiochemical purity, lipophilicity and radiochemical stability of [^{11}C]**3** in various media.

High activities of carbon-11 (> 40 kBq, < 40 MBq) were measured with a calibrated ionization chamber (Atomlab 300; Biodex Medical Systems, Shirley, NY). Low activities of carbon-11 (< 40 kBq) were measured in an automatic γ-counter (Model 1480 Wizard; Perkin-Elmer; Boston, MA) with an electronic window set between 360–1800 keV (counting efficiency, 51.84%). Measurements of carbon-11 were corrected for any significant background and for physical decay with a half-life of 20.385 min.[38]

P-gp knockout mice (*mdr-1a*(−/−)) [39] (model; 001487-MM, double homozygotes) and wild type mice (*mdr-1a*(+/+)) (Model; FVB) were purchased from Taconic Farm (Germantown, NY). Three healthy rhesus monkeys (*Macaca mulatta*) were used in this study. All animal experiments were performed in accordance with the Guide for Care and Use of Laboratory

Animals [40] and were approved by the National Institute of Mental Health Animal Care and Use Committee.

Group data are expressed as mean ± S.D.

4-(4-(4-Chlorophenyl)-4-hydroxypiperidin-1-yl)-2,2-diphenylbutanenitrile (1). 4-(4-Chlorophenyl)-4-hydroxypiperidine (2.12 g, 10.0 mmol) was suspended in acetonitrile (15 mL) and DIPEA (3.5 mL, 30 mmol) added. 4-Bromo-2,2-diphenylbutyronitrile (3.00 g, 10.0 mmol) in acetonitrile (15 mL) was then added. The reaction mixture was stirred under argon at 50 °C for 31 h. After concentration under vacuum, the crude material was re-dissolved in dichloromethane and introduced onto a silica gel column. The product was eluted with ammonium hydroxide solution (2 M) in MeOH: CH_2Cl_2 (6: 94 v/v) to yield **1** as a pale orange solid (3.10 g, 7.21 mmol, 69% yield). M. p. 108−109 °C (n = 3). TLC (silica gel; CH_2Cl_2: 2 M NH_4OH in MeOH (95: 5 v/v); R_f = 0.60. ^{1}H NMR ($CDCl_3$): δ 7.36 (m, 14H), 2.76 (d, J = 11.20 *Hz*, 2H), 2.65 (m, 4H), 2.48 (t, J = 6.9 *Hz*, 2H), 2.08 (t, J = 12.5 *Hz*, 2H), 1.68 (d, J = 11.58 *Hz*, 2H), 1.60 (br s, 1H). ^{13}C NMR ($CDCl_3$): δ 140.16, 132.95, 129.09, 128.57, 128.10, 126.95, 126.23, 122.27, 71.11, 54.93, 50.17, 49.71, 38.52, 36.80. LC-MS (M^++ 1) = 431.2. HRMS (M^++ 1): found 431.1895; calc'd for $C_{27}H_{27}ClN_2O$, 431.1890. LC: 99.89%.

4-(4-(4-Chlorophenyl)-4-hydroxypiperidin-1-yl)-2,2-diphenylbutanamide (2). Compound **1** (2.50 g, 6.00 mmol) was dissolved in ^{t}butanol (20 mL) and potassium hydroxide (1.18 g, 21.0 mmol) was added. The reaction mixture was stirred at 100 °C for 24 h. After concentration under vacuum, the crude material was re-dissolved in dichloromethane and filtered through a pad of celite. Chromatography of the sample on a silica gel column eluted with ammonium hydroxide (2 M) solution in MeOH: CH_2Cl_2 (5: 95 v/v) gave **2** as a pale yellow solid (1.09 g, 2.4 mmol, 37% yield). M. p. = 208−210 °C (n = 3). TLC (silica gel; CH_2Cl_2: 2 M NH_4OH in MeOH (95: 5 v/v); R_f = 0.45. ^{1}H NMR ($CDCl_3$): δ 7.35 (d, J = 4.80 *Hz*, 2 H), 7.26 (m, 12H), 6.49 (s, 1H), 5.51 (s, 1H), 2.77 (d, J = 11.37 *Hz*, 2H), 2.61 (t, J = 7.67 *Hz*, 2H), 2.33 (m, 4H), 2.03 (t, J = 12.64 *Hz*, 2H), 1.70 (br s, 1H), 1.64 (d, J = 11.91 *Hz*, 2H). ^{13}C NMR ($CDCl_3$): δ 176.56, 143.26 132.82, 128.69, 128.41, 127.06, 126.10, 70.90, 59.91, 54.92, 49.48, 38.28, 35.87. LC-MS (M^+ + 1) 449.2. HRMS (M^+ + 1) found 449.2012; calc'd for $C_{27}H_{30}ClN_2O_2$ 449.1996. LC: 99.90%.

4-(4-(4-Chlorophenyl)-4-hydroxypiperidin-1-yl)-2,2-diphenyl-*N*-methyl-butanamide (3). Compound **2** (0.5 g, 1.12 mmol) was dissolved in DMSO (3 mL) at 24 °C and potassium hydroxide (81.2 mg, 1.45 mmol) was added. The reaction was stirred at 80 °C for 24 h. The crude material was injected onto a Luna C18 column (10 μm, 10 × 250 mm; Phenomenex, Torrance, CA) eluted at

8 mL/min with 0.1% CF_3CO_2H: MeCN (72: 28 v/v). The collected fractions were then concentrated under vacuum and re-purified on a silica gel rotor (Chromatotron, Model 7924T, Harrison Research, CA) eluted with ammonium hydroxide solution (2 M) in MeOH: CH_2Cl_2 (5: 95 v/v) to yield **3** as a pale yellow solid (16.5 mg, 0.036 mmol, 3.2% yield). M. p. = 224−226 °C (n = 3). TLC (silica gel; CH_2Cl_2: 2M NH_4OH in MeOH (95: 5 v/v); R_f = 0.45. ^{1}H NMR ($CDCl_3$): δ 7.43 (d, J = 9.2 *Hz*, 2 H), 7.30 (m, 12H), 6.62 (s, 1H), 2.80 (d, J = 4.8 *Hz*, 3H), 2.66 (t, J = 7.2 *Hz*, 2H), 2.39 (m, 4H), 2.08 (t, J = 11.1 *Hz*, 2H), 1.72 (d, J = 11.6 *Hz*, 2H), 1.60 (d, J = 21.2 *Hz*, 2H). ^{13}C NMR ($CDCl_3$): δ 174.79, 143.76, 132.79, 128.77, 128.42, 128.34, 126.91, 126.09, 70.96, 60.10, 58.47, 55.08, 49.50, 26.68. LC-MS, (M^+ + 1) 463.2. HRMS, found (M^+ + 1) 463.2144, calc'd for $C_{28}H_{32}ClN_2O_2$, 463.2152. LC: 99.90%.

Pharmacological Screen of 3. **3** was submitted to the National Institute of Mental Health Psychoactive Drug Screening Program (NIMH-PDSP) for assessment of binding affinity against a wide range of receptors and transporters (5-$HT_{1A,1B,1D,1E,2A–C,3,5A,6,7}$, $\alpha_{1A,2A–2C}$, $\beta_{1,2}$, μ-, κ-, δ-opiate, $D_{1–5}$, $H_{1–3}$, $M_{1–5}$, $\sigma_{1,2}$, NET, SERT and DAT). Detailed assay protocols are available at the NIMH-PDSP web site (http://pdsp.cwru.edu).

Production of [^{11}C]Iodomethane. No-carrier-added [^{11}C]carbon dioxide (~ 38 GBq) was produced in a target of nitrogen gas (~ 164 psi) containing oxygen (1%) via the ^{14}N(p,α)^{11}C reaction induced for 20 min with a 16 MeV proton beam (45 μA) from a PETrace cyclotron (GE; Milwaukee, WI). [^{11}C]Iodomethane was produced within a lead-shielded hot-cell from the [^{11}C]carbon dioxide via reduction to [^{11}C]methane and iodination[41] within a MeI MicroLab apparatus (GE).

Preparation of [^{11}C]3. Radiochemistry was performed in a PLC-controlled semi-robotic Synthia apparatus[42] (Synthia, Uppsala, Sweden), housed within the same lead-shielded hot-cell used to prepare [^{11}C]iodomethane. [^{11}C]Iodomethane in carrier helium (15 mL/min) was bubbled into a sealed 1 mL-vial containing **2** (1.0 mg, 2.23 μmol) and KOH (5.0 mg, 89.3 μmol) in DMSO (0.4 mL). When the radioactivity in the vial had maximized, the reaction mixture was heated at 80 °C for 5 min and then diluted with water (500 μL). The crude material was injected onto a Gemini C18 column (5 μm, 10 × 250 mm; Phenomenex) eluted at 6 mL/min with ammonium hydroxide solution (2 M) in MeOH: CH_2Cl_2 (62: 38 v/v). Eluate was monitored for radioactivity (pin diode detector HC-003; Bioscan) and absorbance at 225 nm (Gold 166 detector; Beckman). [^{11}C]**3** (R_t = 10.2 min) eluted after **2** (R_t = 8.71 min) and was collected in a 10-mL round-bottom vial containing *aq.* ascorbic acid (0.11

Comment [p1]: Detectors?

mM; USP grade), diluted with sterile saline (10 mL), and filtered through a sterile filter (Millex MP, Millipore, Bedford, MA).

[^{11}C]**3** was analyzed for radiochemical purity on a Luna C18 column (5 μm, 10 × 250 mm; Phenomenex) eluted with 0.1% CF_3CO_2H: MeCN (40: 60 v/v) at 2.5 mL/min (t_R = 5.55 min), with eluate monitored for absorbance at 225 nm (Gold 166 detector, Beckman) and radioactivity. The identity of [^{11}C]**3** was confirmed by i) LC-MS-MS of associated carrier, and ii) observation of co-elution with added authentic **3** in a second radio-HPLC analysis.

Computation of *cLogP* and *cLogD,* and Measurement of *LogD*. *cLogP* and *cLogD* (at *pH* = 7.4) values for **3** were computed with the program Pallas 3.0 for Windows (CompuDrug; S. San Francisco; CA).

The *LogD* value of [^{11}C]**3** was determined by measuring its distribution between *n*-octanol and sodium phosphate buffer (0.15 M, *pH* 7.4), as previously described for other radiotracers.[43,44]

PET Imaging of [^{11}C]3 in Mouse Brain. Brains of mice were scanned with the Advanced Technology Laboratory Animal Scanner (ATLAS). This small-animal PET camera has effective transaxial and axial fields of view of 6.0 and 2.0 cm, respectively.[45] Mice were anaesthetized with 1.5% isoflurane in oxygen, and body temperatures maintained between 36.5 and 37.0 °C with a

heating pad or lamp. Radiotracer was injected via a polyethylene cannula (PE-10; Becton Dickinson, Franclin Lakes, NJ) secured in the mouse tail vein with tissue adhesive (Vetbond; 3M, St. Paul, MN).

On three occasions, one P-gp knockout mouse (19−23.8 g) and one wild type mouse (28.6−29.5 g) were placed in the camera gantry and each injected with a bolus of [^{11}C]**3** (2.11−2.79 MBq; SA 40.7−131 GBq/μmol). The injected radioactivities gave count rates within the linear range of scanner performance i.e. < 300,000 singles per s. Scans were obtained from the time of injection for 90 min in the frame sequence 6 × 20 s, 5 × 1 min, 4 × 2 min, 3 × 5 min and 3 × 10 min. Data were corrected for random events and detector efficiency. Images were reconstructed with a 3D ordered-subset expectation maximization algorithm into 17 coronal slices with 3 iterations and 16 subsets, resulting in a resolution of about 1.6 mm full width at half maximum (fwhm).[46,47] The reconstructed voxel size was 0.56 × 0.56 × 1.12 mm. No attenuation or scatter correction was applied.

Images were analyzed with pixel-wise modeling software (PMOD Group; Zurich, Switzerland). Two regions of interest (ROIs), forebrain and cerebellum, were drawn on coronal slices guided by a mouse brain stereotaxic atlas.[48] Brain uptake of radioactivity was corrected for decay and normalized

for injected dose and body weight by expression as percent standardized uptake value (%SUV), defined as:

%SUV = [(activity per g tissue)/injected activity] × g body weight × 100.

Measurement of [^{11}C]3 and Radiometabolites in Mouse Plasma and Brain. Thirty minutes after injection of [^{11}C]**3** into each of three wild type and three knockout mice, anti-coagulated blood (1 mL) was sampled by cardiac puncture. Plasma (~ 100−450 μL) was separated by centrifugation, deproteinized with acetonitrile (700 μL) and measured for radioactivity in an automatic γ-counter.[49] The animals were decapitated, and forebrains and cerebella removed for immediate radioanalysis.[49] Brain-tissue radioactivities were measured in the γ-counter. Brain tissue suspension, along with carrier **3**, was homogenized in 1.5 times its volume of acetonitrile with a hand-held tissue Tearor (model 985-370; BioSpec Products Inc.). Water (500 μL) was added and the mixture homogenized again. Homogenates were then centrifuged at 10,000 *g* for 1 min. The resulting precipitates and supernatant liquids were measured for radioactivity to allow the recovery of activity into the acetonitrile supernatants to be calculated. Aliquots of the clear pre-filtered supernatant liquids were analyzed by radio-HPLC (see general methods).

PET Imaging of Monkey Brain with [^{11}C]3. One male rhesus monkey (A; 8.37 kg) was fasted overnight, immobilized with ketamine (10 mg/kg, i.m.),

intubated, placed on a ventilator, and anesthetized with 1.6% isoflurane in O_2. Body temperature was maintained between 36.5 and 37.0 °C. After injecting [^{11}C]**3** (211 MBq in 4-5 mL) through an intravenous perfusion line, filled with saline, dynamic PET scans of the brain were acquired on an HRRT camera (Siemens, Knoxville, TN) for 120 min in 33 frames of duration increasing from 30 s to 5 min. Images were reconstructed using filtered back-projection in list mode 3D-OSEM,[50] resulting in a resolution of 2.5 mm fwhm. Scatter and attenuation correction were applied. ROIs were drawn on coronal slices. Images were analyzed with PMOD 2.5 (pixel-wise modeling software; PMOD Group, Adliswil, Switzerland). Activity was decay-corrected to the time of injection and expressed as %SUV.

Three hours after the baseline scan, P-gp was blocked with DPCQ (8 mg/kg. i.v.) in the same monkey and the scanning repeated. For this purpose DPCQ (67.3 mg, 0.120 mmol) was dissolved with the aid of sonication in sterile aqueous mannitol (5% w/v; 10 mL), diluted with sterile saline (10 mL) and finally passed through a sterile filter (Anatop 25; 0.2 μm, 25 mm; Whatman). This DCPQ solution (3.36 mg/mL; 19.76 mL) was infused into the monkey over 10 min. After 20 min the monkey was injected with [^{11}C]**3** (218 MBq).

The baseline and P-gp blocked experiments were repeated in a second monkey (B; 12.45 kg) with naloxone (5 mg, i.v.) administered at 30 min after

the second injection of [^{11}C]**3** and in another monkey (C; 15.72 kg) in which the dose of DCPQ was increase to 16 mg/kg (i.v.) and the naloxone was given as before. Injected activities in this sequence of experiments were 313, 283, 377 and 355 kBq, respectively.

Emergence of Radiometabolites of [^{11}C]3 in Monkey Plasma. After the administration of [^{11}C]**3** to monkey (A) under baseline and P-gp blocked condition (achieved with DCPQ at 8 mg/kg, i.v.), eight arterial blood samples (0.5 mL each) were drawn into heparin-treated syringes at 15 s intervals until 2 min, followed by 1 mL aliquots at 3, 5, 10, 20, 30, 45, 60, 75, 90 and (in DCPQ-treated monkey only) 120 min. Samples were measured for radioactivity. Plasma [^{11}C]**3** was separated, measured for radioactivity, deproteinized and the [^{11}C]**3** and radiometabolite contents quantified with radio-HPLC (general method A).

Acknowledgements. This research was supported by Intramural Research program of the National Institutes of Health (National Institute of Mental Health). We are grateful to the NIH Clinical Research Center PET Group for radionuclide production and for assistance on PET Imaging, to PMOD Technologies for providing the image analysis software and the NIMH Psychoactive Drug Screening Program (PDSP) for performing assays; the PDSP is directed by Bryan L. Roth, PhD with project officer Jamie Driscol

(NIMH), at the University of North Carolina at Chapel Hill (contract # NO1MH32004). We are also grateful to GlaxoSmithKline for a gift of reference **3** and to Eli Lilly for DCPQ.

References

(1) Tsuji, A; Tamai, I. Blood−brain barrier function of P-glycoprotein. *Adv. Drug Delivery Rev.*, **1997**, *25*, 287-298.

(2) Cordon-Cardo, C.; O'Brien, J. P.; Boccia, J.; Casals, D.; Bertino, J. R.; Melamed, M. R. Expression of the multidrug resistance gene product (P-glycoprotein) in human normal and tumor tissues. *J. Histochem. Cytochem.* **1990**, *9*, 1277-1287.

(3) Schinkel, A.; Wagenaar, E.; Mol, C.; van Deemter, L. P-glycoprotein in the blood-brain barrier of mice influences the brain penetration and pharmacological activity of many drugs. *J. Clin. Invest.* **1996**; *97*: 2517−2524.

(4) Kim, R. B.; Fromm. M. F.; Wandel, C.; Leake; B.; Wood, A. J. J.; Roden, D. M.; Wilkinson, G. R. The drug transporter P-glycoprotein limits oral absorption and brain entry of HIV-1 protease inhibitors. *J. Clin. Invest.* **1998**, *101*, 289–94

(5) Gottesman, M.; Fojo, T.; Bates, S. Multidrug resistance in cancer: role of ATP-dependent transporters. *Nat. Rev. Cancer.* **2002**, *2*, 48-58.

(6) Lam, F. C.; Liu, R.; Lu, P.; Shapiro, A. B.; Renoir, M.; Sharom, F. J.; Reiner, P. B. β-Amyloid efflux mediated by P-glycoprotein. *J. Neurochem*. **2001**, *76*, 1121-1128.

(7) Cirrito, J. R.; Deane, R.; Fagan, A. M.; Spinner, M. L.; Parsadanian, M.; Finn, M. B.; Jiang, H.; Prior, J. L.; Sagare, A.; Bales K R., Paul S. M.; Zlokovic, B. V.; Piwnica-Worms, D.; Holtzman, D. M. P-Glycoprotein deficiency at the blood-brain barrier increases amyloid-β deposition in an Alzheimer disease mouse model. *J. Clin. Invest*. **2005**, *115*, 3285-3290.

(8) Vogelgesang, S.; Cascorbi, I.; Schroeder, E.; Pahnke, J.; Kroemer, H. K.; Siegmund, W.; Kunert-Keil, C.; Walker, L. C.; Warzok, R. W. Deposition of Alzheimer's β-amyloid is inversely correlated with P-glycoprotein expression in the brains of elderly non-demented humans. *Pharmacogenetics*, **2002**, *12*, 535-541.

(9) Langford, D.; Grigorian, A.; Hurford, R.; Adame, A.; Ellis, R. J.; Hansen, L.; Masliah E. Altered P-glyocoprotein expression in AIDS patients with HIV encephalitis. *J. Neuropath. Exp. Neurology*, **2004**, *63*, 1038-1046.

(10) Kortekaas, R.; Leenders, K. L.; van Oostrom, J. C. H.; Vaalburg, W.; Bart, J.; Willemsen, A. T. M.; Hendrikse, N. H. Blood-brain barrier dysfunction in Parkinsonian midbrain in vivo *Ann. Neurol.* **2005**, *57*, 176-179.

(11) Liow, J. S.; Lu, S.; McCarron, J. A. ; Hong, J., Musachio, J. L.; Pike, V. W.; Innis, R. B.; Zoghbi, S. S. Effect of a P-glycoprotein inhibitor, cyclosporin A, on the disposition in rodent brain and blood of the 5-HT_{1A} receptor radioligand, [^{11}C](*R*)-(−)-RWAY. *Synapse* **2007**, *96*, 96−105.

(12) Elsinga, P. H.; Hendrikse, N. H.; Bart, J.; van Waarde, A.; Vaalburg, W. Positron emission tomography studies of central nervous system drugs and P-glycoprotein function in the rodent brain. *Mol. Imaging Biol.* **2005**, *7*, 37-44.

(13) Elsinga, P. H.; Hendrikse, N. H.; Bart, J.; Vaalburg, W.; van Waarde, A. PET studies on P-glycoprotein function in the blood-brain barrier: how it affects uptake and binding of drugs within the CNS. *Curr. Pharm. Design* **2004**, *10*, 1493−1503.

(14) Levchenko, A.; Mehta, B.; Lee, J.; Humm, J. L.; Augensen, F.; Squire, O.; Kothari, P. J.; Finn, R. D.; Leonard, E. F.; Larson, S. M. Evaluation of ^{11}C-colchicine for PET imaging of multiple drug resistance. *J. Nucl. Med.* **2000**, *41*, 493−501.

(15) Elsinga, P. H.; Franssen, E. J. F.; Hendrikse, N. H.; Fluks, L.; Weemaes, A. M. A.; van der Graaf, W. T. A.; deVries, G. E.; Visser, G. M.; Vaalburg, W. Carbon-11-labeled daunorubicin and verapamil for probing P-glycoprotein in tumors with PET. *J. Nucl. Med.* **1996**, *37*, 1571−1575.

(16) Takano, A.; Kusuhara. H.; Suhara. T.; Ieiri, I.; Morimoto, T.; Lee, Y. J.; Maeda, J.; Ikoma, Y.; Ito, H.; Suzuki, K.; Sugiyama, Y. Evaluation of in vivo P-glycoprotein function at the blood–brain barrier among MDR1 gene polymorphisms by using ^{11}C-verapamil. *J. Nucl. Med.* **2006**, *47*, 1427−1433.

(17) Kurdziel, K.; Kiesewetter, D.; Carson, R.; Eckelman, W.; Herscovitch, P. Biodistribution, radiation dose estimates, and in vivo Pgp modulation studies of ^{18}F-paclitaxel in nonhuman primates. *J. Nucl. Med.* **2003**, *44*, 1330−1339.

(18) Bigott, H.; Prior, J.; Piwnica-Worms, D.; Welch, M. Imaging multidrug resistance P-glycoprotein transport function using microPET with technetium-94m-sestamibi. *Mol. Imaging.* **2005**, *4*, 30−39.

(19) Passchier. J.; Bender, D.; Matthews, J. C.; Lawrie, K. W.; Gee, A. D. [^{11}C]Loperamide: a novel and sensitive PET probe for quantification of changes in P-glycoprotein functionality. *Mol. Imaging Biol.* **2003**, *5*, 121 (abstract).

(20) Wilson, A. A.; Passchier, J.; Garcia, A.; Vasdev, N.; Stableford, W.; Lawrie, K.; Fellows, I.; Gee, A. D. Production of the P-glycoprotein

marker [^{11}C]loperamide, in clinically useful quantities. *J. Labelled Compd. Radiopharm*. **2005**, 48, S142 (abstract).

(21) Del Vecchio, S.; Ciarmiello, A.; Potena, M.; Carriero, M. V.; Mainolfi, C.; Botti, G.; Thomas, R.; Cerra, M.; Daiuto, G.; Tsuruo, T.; Salvatore, M. In vivo detection of multidrug-resistant (MDR1) phenotype by technetium-99m sestamibi scan in untreated breast cancer patients. *Eur. J. Nucl. Med.* **1997**, *24*, 150−159.

(22) Awouters, F.; Megens, A.; Verlinden, M.; Schuurkes, J.; Niemegeers, C.; Janssen, P. A. J. Loperamide – survey of studies on mechanism of its antidiarrheal activity. *Digestive Diseases and Sciences* **1993**, *38*, 977-995.

(23) Sadeque, A. J. M.; Wendel, C.; He, H. B.; Shah S.; Wood, A. J. J. Increased drug delivery to the brain by P-glycoprotein. *Clin. Pharmacol. Therapeutics*, **2000**, *68*, 231-237.

(24) Zoghbi, S. S.; Liow, J.-S.; Yasuno, F.; Hong, J.; Tuan, E.; Lazarova, N.; Gladding, R. L.; Pike, V. W.; Innis, R. B. ^{11}C-Loperamide and its *N-desmethyl* radiometabolite are avid substrates for brain P-glycoprotein efflux. *J. Nucl. Med*. In press.

(25) Kalgutkar, A. S.; Nguyen, H. T. Identification of *N*-methyl-4-phenylpyridinium-like metabolite of the antidiarrheal agent loperamide in

human liver microsomes: underlying reason(s) for the lack of neurotoxicity despite the bioactivation event. *Drug Metab. Dispos*. **2004**, *32*, 943−952.

(26) Yoshida, K.; Nambu, K.; Arakawa, S.; Miyazaki, H.; Hashimoto, M. Metabolism of loperamide in rats. *Biomed. Mass Spectrom.* **1979**, *6*, 253−259.

(27) Stokbroekx. R. A.; Vandenberk, J.; Van Heertum, A. H. M. T.; Van Laar, G. M. L. W.; Van der Aa, M. J. M. C.; Van Bever, W. F. M.; Janssen, P. A. J. Synthetic antidiarrheal agents. 2,2-Diphenyl-4-(4'-aryl-4'-hydroxypiperidino)butyramides. *J. Med. Chem.* **1973**, *16*, 782-786.

(28) Pike, V. W. Positron-emitting radioligands for studies in vivo – probes for human psychopharmacology. *J. Psychopharmacol*. **1993**, *7*, 139-158.

(29) Waterhouse, R. N. Determination of lipophilicity and its use as a predictor of blood-brain barrier penetration of molecular imaging agents. *Mol. Imaging Biol.* **2003**, *5*, 376-389.

(30) Stahl, K. D.; Van Bever, W.; Janssen, P.; Simon, E. J. Receptor affinity and pharmacological potency of a series of narcotic analgesic, anti-diarreal and neuroleptic drugs. *Eur. J. Pharmacol*. **1977**, *46*, 199-205.

(31) Shepard, R. L.; Cao, J.; Starling, J. J.; Dantzig, A. H. Modulation of P-glycoprotein but not MRP1- or BCRP-mediated drug resistance by LY335979. *Int. J. Cancer* **2003**, *103*, 121 -125.

(32) Dantzig, A. H.; Shepard, R. L.; Law, K. L.; Tabas, L.; Pratt, S.; Gillespie, J. S.; Binkley, S. N.; Kuhfeld, M. T.; Starling, J. J.; Wrighton, S. A. Selectivity of the multi-drug resistance modulator, LY335979, for P-glycoprotein and effect on cytochrome P450 activities. *JPET* **1999**, *290*, 854-890.

(33) Jones, A. K. P.; Luthra, S. K.; Maziere, B.; Pike, V. W.; Loc'h, C.; Crouzel, C.; Syrota, A.; Jones, T. Regional cerebral opioid receptor studies with [^{11}C]diprenorphine in normal volunteers. *J. Neurosci. Methods* **1988**, *23*, 121-129.

(34) Shiue, C. Y.; Bai, L. Q.; Teng, R. R.; Arnett, C. D.; Dewey, S. L.; Wolf, A. P.; McPherson, D. W.; Fowler, J. S.; Logan, J.; Holland, M. J.; Simon E. J. A comparison of the brain uptake of *N*-(cyclopropyl[^{11}C]methyl norbuprenorphine ([^{11}C]buprenorphine) and *N*-(cyclopropyl[^{11}C]methyl nordiprenorphimne ([^{11}C]diprenorphine) in baboon using PET. *Nucl. Med. Biol*. **1991**, *18*, 281-288.

(35) Talbot, P. S.; Narendran, R.; Butelman, E. R.; Huan, Y. Y.; Ngo, K.; Slifstein, M., Martinez, D.; Laruelle, M.; Hwang, D. R. [^{11}C]GR103545,

a radiotracer for imaging kappa-opioid receptors in vivo with PET: synthesis and evaluation in baboons. *J. Nucl. Med.* **2005**, *46*, 484-494.

(36) Madar, I.; Bencherif, B.; Lever, J.; Heitmiller, R. F.; Yang, S. C.; Brock, M.; Brahmer, J.; Ravert, H.; Dannals, R.; Frost, J. J. Imaging delta- and mu-opioid receptors by PET in lung carcinoma patients. *J. Nucl. Med*. **2007**, *48*, 207-213.

(37) Pfister, J. R.; Makra, F.; Muehldorf, A. V.; Wu, H.; Nelson, J. T.; Cheung, P.; Bruno, N. A., Casey, S. M.; Zutshi, N.; Slate, D. L. Methanodibenzsuberylpiperazines as potent multidrug resistance reversal agents. *Bioorg. Med. Chem. Lett.* **1995**, *5*, 2473-2476.

(38) Weber, D. A.; Eckerman, K. F.; Dillman, L. T.; Ruyman, J. C. *MIRD*: *Radionuclide Data and Decay Schemes*. New York: Society of Nuclear Medicine. **1989**, 447.

(39) Schinkel, A. H.; Smit, J. J. M.; Vantellingen, O.; Belinen, J. H.; Wagenaar, E.; Vandeeemter, L.; Mol, C. A. A. M.; Vandervalk, M .A.; Robanusmaandag, E. C.; Teriele, H. P. J.; Berns, A. J. M.; Borst, P. Disruption of the mouse mdr1a P-glycoprotein gene leads to a deficiency in the blood-brain barrier and to increased sensitivity to drugs. *Cell* **1994**, *77*, 491−502.

(40) Clark, J. D.; Baldwin, R. L.; Bayne, K. A.; Brown, M. J.; Gebhart, G. F.; Gonder, J. C.; Gwathmey, J. K.; Keeling, M. E.; Kohn, D. F; Robb, J. W.; Smith, O. A.; Steggerda, J.-A. D.; VandeBer, J. L. *Guide for the Care and Use of Laboratory Animals*. Washington D.C: National Academy Press, 1996.

(41) Larsen, P.; Ulin, J.; Dahlstrøm, K.; Jensen, M. Synthesis of [^{11}C]iodomethane by iodination of [^{11}C]methane. *Appl Radiat Isot.* **1997**, *48*, 153-157.

(42) See http://www.uppsla.imanet.se/research-synthia.asp for a description of similar apparatus.

(43) Zoghbi, S. S.; Baldwin, R. M.; Seibyl, J. P.; Charney, D. S., Innis, R. B. A radiotracer technique for determining apparent pKa of receptor-binding ligands. *J. Labelled Compd. Radiopharm.* **1997**; *40SI*, 136-138.

(44) Briard, E.; Zoghbi, S. S.; Imaizumi, M.; Gourley, J. P.; Shetty, H. U.; Hong, J.; Cropley, V.; Fujita, M.; Innis, R. B.; Pike V. W. Synthesis and evaluation in monkey of two sensitive ^{11}C-labeled aryloxyanilide ligands for imaging brain peripheral benzodiazepine receptors in vivo. *J. Med. Chem*. In press.

(45) Seidel, J.; Vaquero, J. J.; Green, M. V. Resolution uniformity and sensitivity of the NIH ATLAS small animal PET scanner: comparison to

simulated LSO scanners without depth-of-interaction capability. *IEEE Trans. Nucl. Sci*. **2003**, *50*, 1347–1350.

(46) Johnson, C. A.; Seidel, J.; Vaquero, J. J.; Pascau, J.; Desco, M.; Green, M. V. Exact positioning for OSEM reconstructions on the ATLAS depth-of interaction small animal scanner. *Mol. Imaging Biol*. **2002**; *4*: S22 (abstract).

(47) Liow, J.; Seidel, J.; Johnson, C. A.; Toyama, H.; Green, M. V.; Innis, R. B. A single slice rebinning/2D exact positioning OSEM reconstruction for the NIH ATLAS small animal PET scanner. *J. Nucl. Med.* **2003**, *44*, 162P (abstract).

(48) Paxinos, G.; Watson, C. *The Rat Brain in Stereotaxic Coordinates,* 6th Edition, Amsterdam, Boston, Elsevier 2001.

(49) Zoghbi, S. S.; Shetty, U. H.; Ichise M.; Fujita, M.; Imaizumi, M.; Liow, J.-S.; Shah, J.; Musachio, J. L.; Pike, V. W.; Innis, R. B. PET imaging of the dopamine transporter with [^{18}F]FECNT: a polar radiometabolite confounds brain radioligand measurements. *J. Nucl. Med.* **2006**, *47*, 520−527.

(50) Carson, R. E.; Barker, W. C.; Liow, J.-S. Johnson, C. A. *Conference Record of the IEEE Nuclear Science Symposium and Medical Imaging Conference*; Portland, Oregon, 2003.

Table 1. Radioactivity content in brain tissue and plasma and its distribution at 30 min after administration of [^{11}C]**3** to wild type and P-gp knockout mice. Values are mean ± SD (n = 3).

Mice	Tissue	Total radioactivity	Radioactivity distribution (%)			
		(%SUV)	[^{11}C]**3**	[^{11}C]A	[^{11}C]B	[^{11}C]C
WT	Cerebellum	5.6	45.5 ± 6.7	42.4 ± 2.4	8.2 ± 5.0	3.9 ± 2.1
	Forebrain	5.4	43.6 ± 5.5	41.4 ± 3.3	11.7 ± 2.4	3.3 ± 0.5
	Plasma	25.3	11.1 ± 0.7	67.5 ± 13.2	20.9 ± 13.6	0.5 ± 0.3
KO	Cerebellum	44.4	88.9 ± 4.2	3.5 ± 0.9	1.2 ± 0.7	6.4 ± 3.1
	Forebrain	38.9	91.3 ± 3.6	3.6 ± 1.9	0.8 ± 0.5	4.3 ± 2.3
	Plasma	22.1	7.9 ± 1.6	58.0 ± 27.5	33.7 ± 29.3	0.3 ± 0.2

Comment [p2]: Sami please check and provide missiing data

Scheme 1. Synthesis of **2**, **3**, and radiotracer [^{11}C]**3**.[a]

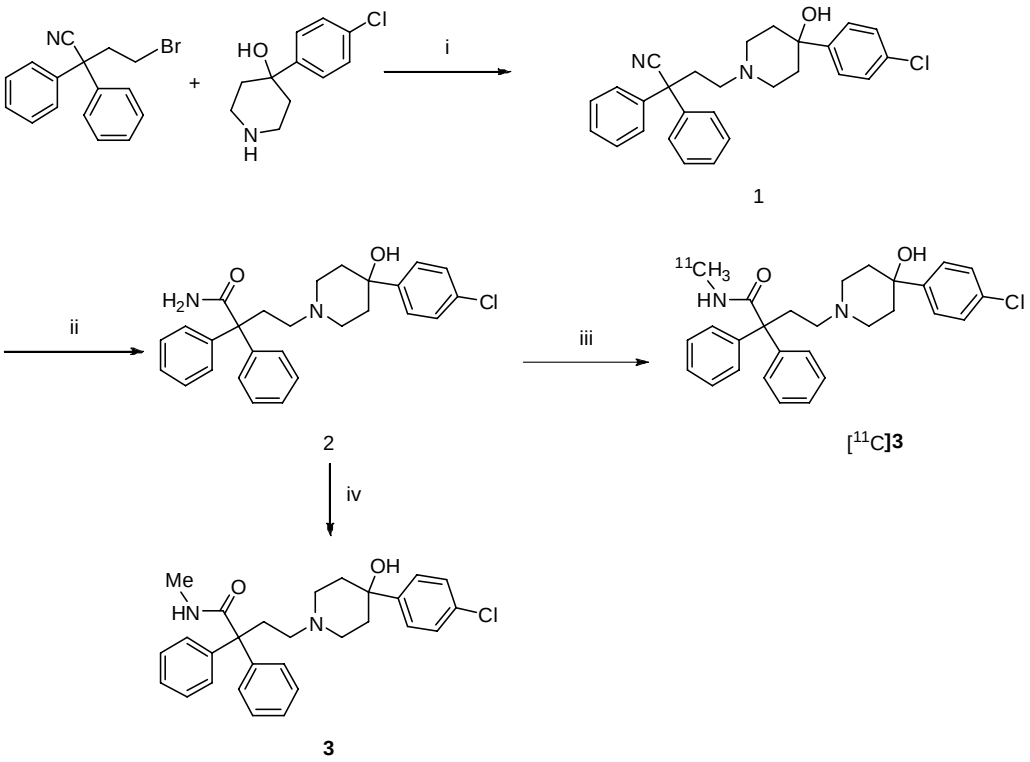

[a] Reagents, conditions and yields: (i) DIPEA, MeCN, 70 °C, 31 h , yield 69%; (ii) KOH, ^{t}BuOH, 100 °C, 3 d, yield 37%; (iii) [^{11}C]MeI, KOH, DMSO, 80 °C, 5 min, RCY 18% from [^{11}C]carbon dioxide; (iv) MeI, KOH, DMSO, 80 °C, 24 h, 3%.

Legends to Figures

Figure 1. Structures of loperamide and *N-desmethyl*-loperamide (dLop; **3**).

Figure 2. Chromatograms from the HPLC separation of [^{11}C]**3**. See Methods for chromatographic conditions.

Figure 3. Time-activity curves in forebrain (Panel A) and cerebella (Panel B) of three P-gp knockout and three wild type mice measured with PET after the intravenous administration of [^{11}C]**3**. Key: wild type cerebellum (○); knockout cerebellum (□); wild type forebrain (●); knockout forebrain (■). Error bars are S.D. values (n = 3).

Figure 4. Radiochromatogram of radioactive species in P-gp knockout mouse forebrain at 30 min after the administration of [^{11}C]**3**. See Methods for full chromatographic conditions.

Figure 5. Regional uptake of radioactivity in monkey brain after the administration of [^{11}C]**3** under baseline conditions (Panel A) , and at 20 min after the administration of DCPQ (8 mg/kg, i.v.) (Panel B). Key: frontal cortex (▽), temporal cortex (○), parietal cortex (◇), putamen (×), cerebellum (□) and pituitary (●).

Figure 6. Summed transaxial PET images obtained at 20 to 90 min after the intravenous administration of [^{11}C]**3** to monkey under baseline conditions (Panel A) and after P-gp inhibition with DCPQ (8 mg/kg, i.v.) (Panel B).

Figure 7. Uptake of radioactivity into monkey brain regions after administration of [^{11}C]**3** at 20 min after administration of DCPQ (16 mg/kg), with naloxone (5 mg/kg, i.v.) given at 30

min after radioligand injection. Key: frontal cortex (●), anterior cingulate (+), temporal cortex (▽), parietal cortex (◇), hippocampus (*), occipital cortex (□), putamen (△) and cerebellum (×).

Figure 8. Pituitary uptake of radioactivity after intravenous administration of [^{11}C]**3** to monkey under baseline conditions (○), under conditions in which P-gp was inhibited with DCPQ (8 mg/kg i.v.) with naloxone (5 mg/kg, i.v.) given at 30 min after radiotracer (□), and under conditions in which P-gp is inhibited with DCPQ (16 mg/kg, i.v.) with the naloxone given as before (△).

Figure 9. Whole blood radioactivity concentration after administration of [^{11}C]**3** to monkey under baseline conditions (□) or at 20 min after administration of DCPQ (8 mg/kg, i.v.) (○).

Figure 10. Concentration of unchanged [^{11}C]**3** in plasma after administration to monkey under baseline condition (○) and at 20 min after inhibition of P-gp with DCPQ (8 mg/kg, i.v.) (●).

Figure 11. Time course of composition of radioactivity in plasma after intravenous administration of [^{11}C]**3** into monkey under baseline conditions (Panel A) and at 20 min after administration of DCPQ (x mg/kg, i.v.) (Panel B). Key: [^{11}C]**3** (●); [^{11}C]A (△); [^{11}C]B (▽); [^{11}C]C (◇); unextracted for analysis (□).

Figure 12. Structures of DCPQ and Zosuquidar

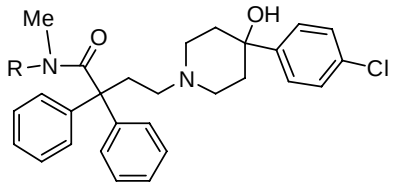

R = Me, Loperamide
R = H, *N*-Desmethylloperamide (**3,** dLop)

Figure 1.

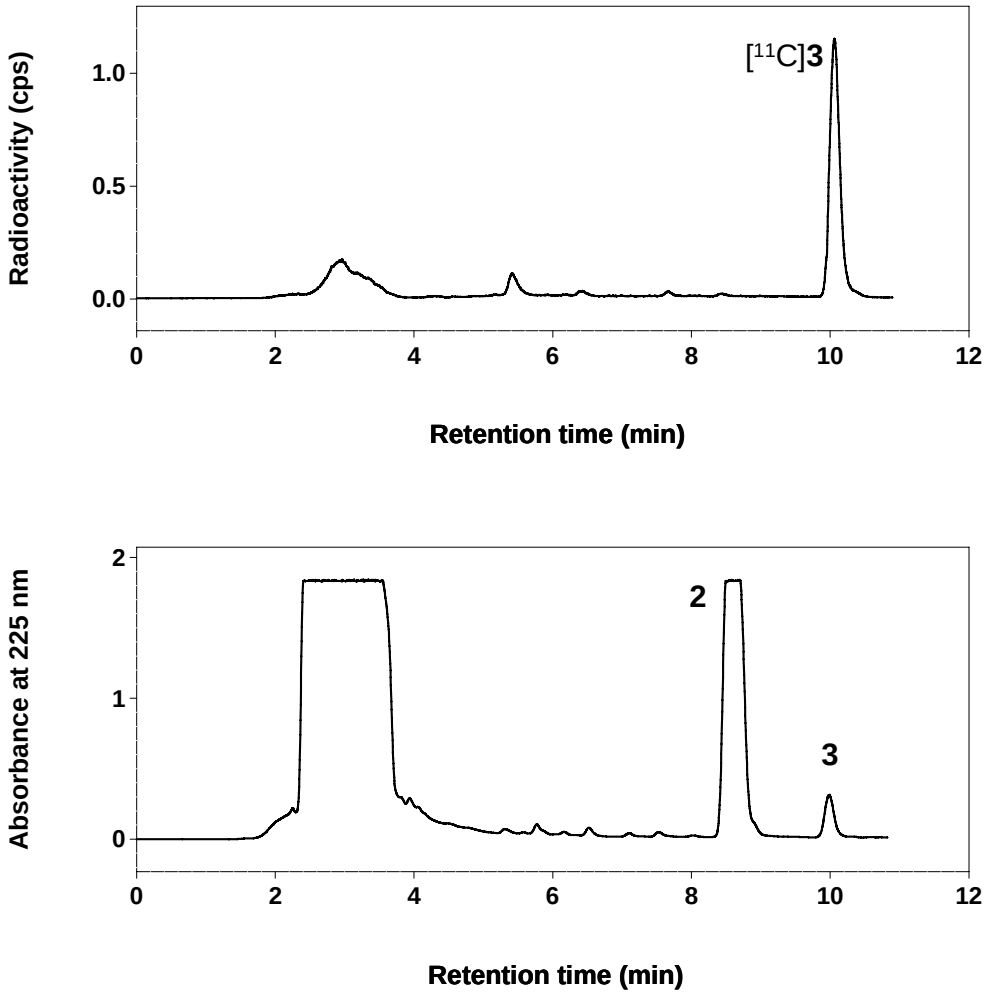
Radioactivity (cps)
1.0
0.5
0.0
[11C]3
0
2
4
6
8
10
12
Retention time (min)
Absorbance at 225 nm
2
1
0
2
3
0
2
4
6
8
10
12
Retention time (min)

Figure 2.

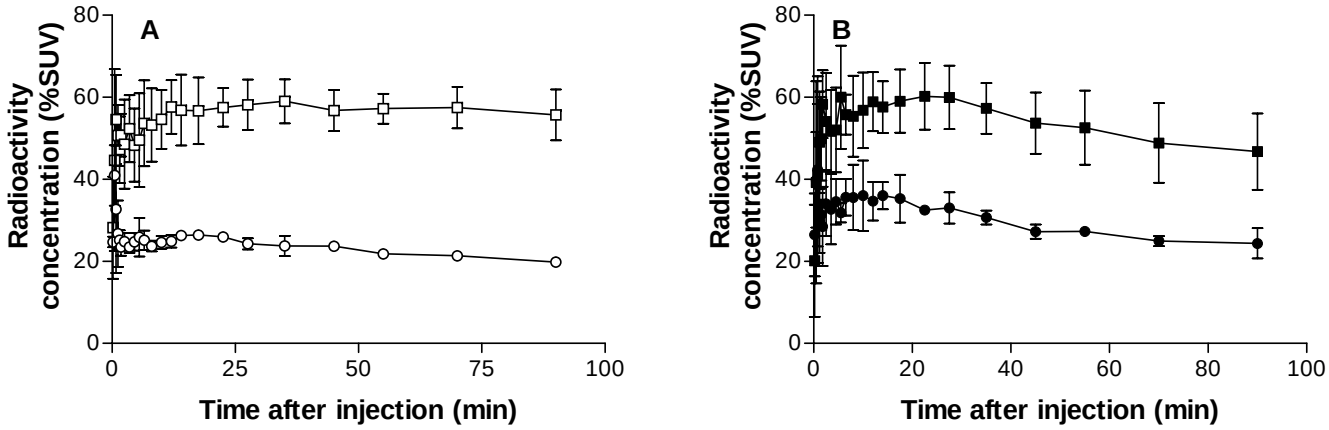
A
B
Radioactivity concentration (%SUV)
Time after injection (min)
0
20
40
60
80
100
0
25
50
75

Figure 3.

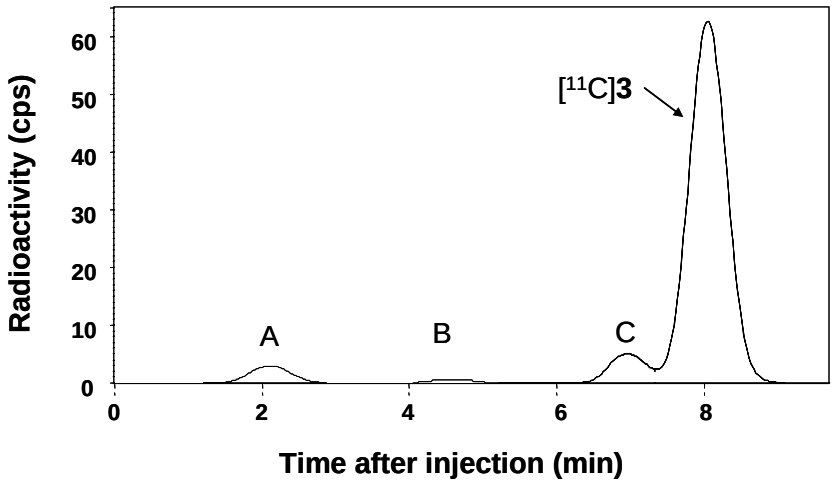
Radioactivity (cps)
60
50
40
30
20
10
0
A
B
C
[11C]3
0
2
4
6
8
Time after injection (min)

Figure 4.

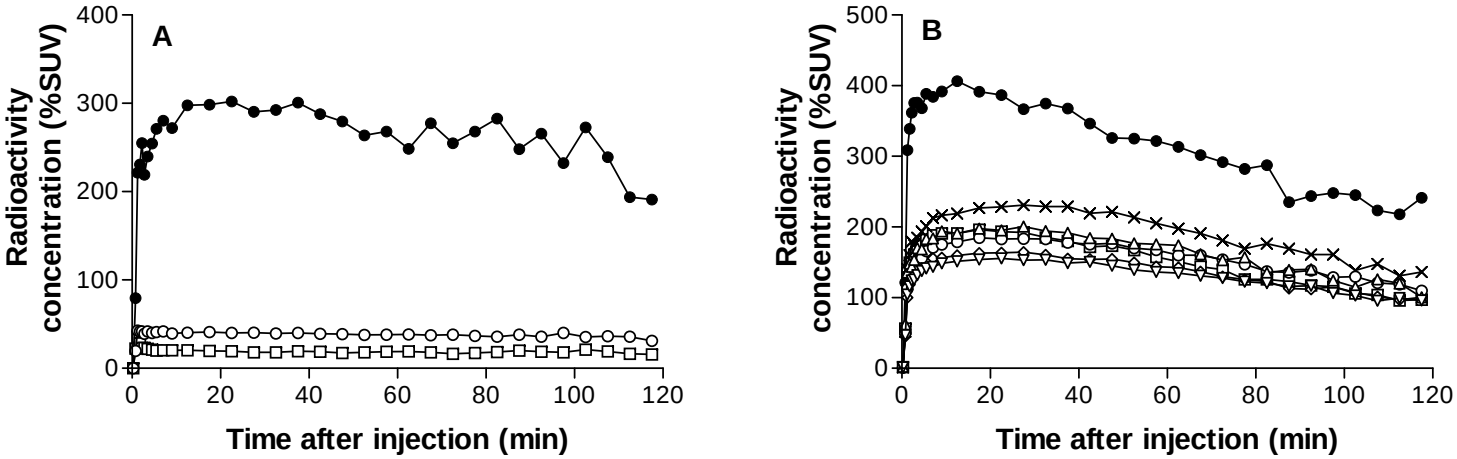
A
B
Radioactivity concentration (%SUV)
Time after injection (min)
0
100
200
300
400
500
0
20
40
60
80
100
120

Figure 5.

Comment [p3]: Sami please provide data on cerebellum to be added into this figure

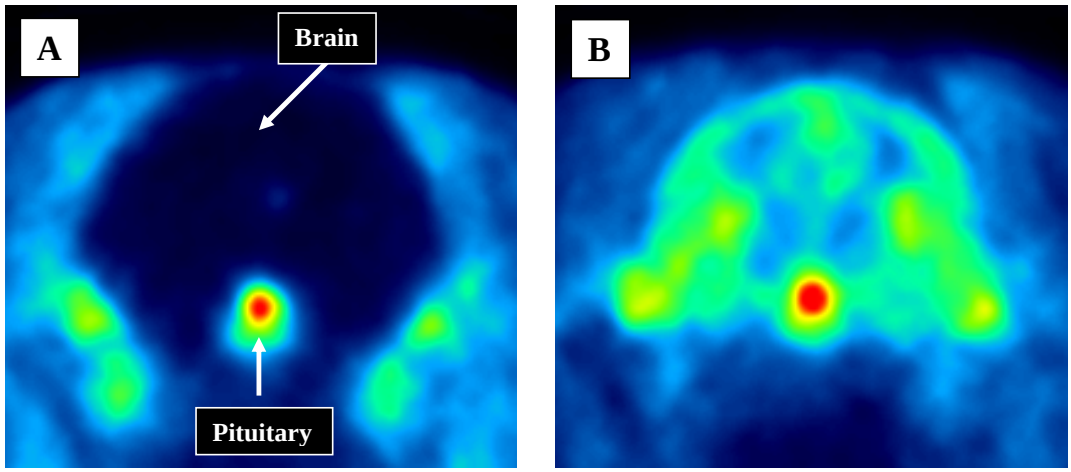

Figure 6.

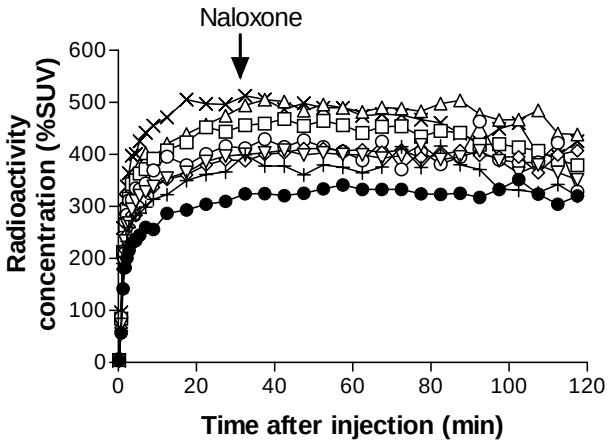
Naloxone
Radioactivity concentration (%SUV)
600
500
400
300
200
100
0
0
20
40
60
80
100
120
Time after injection (min)

Figure 7.

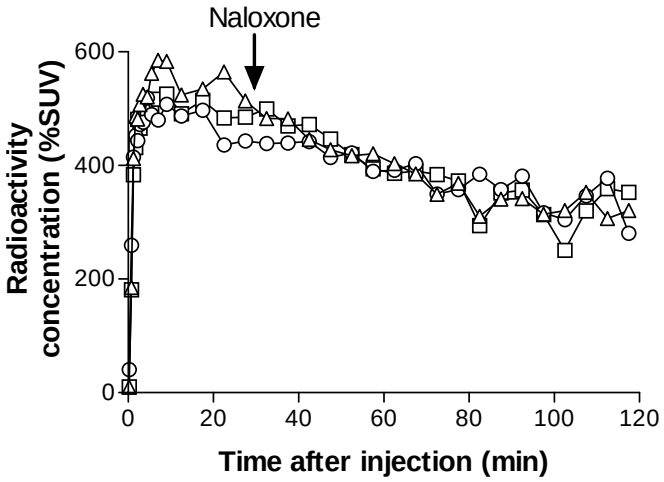
Naloxone
600
400
200
0
Radioactivity concentration (%SUV)
0
20
40
60
80
100
120
Time after injection (min)

Figure 8.

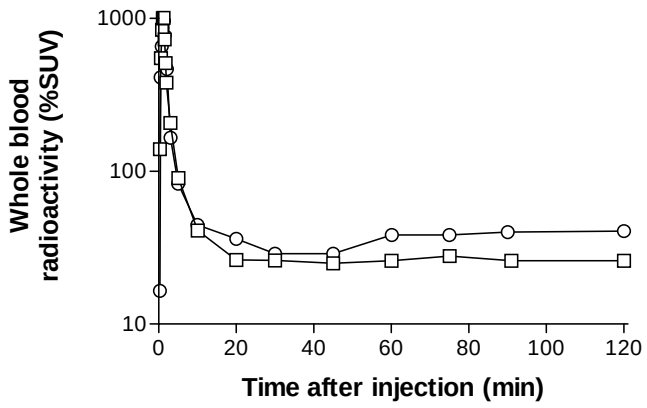

Comment [p4]: Jeih-San please provide a color scale and delineate brain within the scan. Also state how image was obtained – by summation over???

Figure 9.

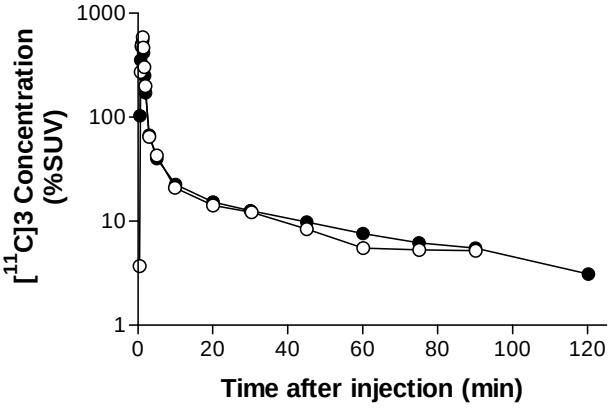
1000
100
10
1
[11C]3 Concentration (%SUV)
0
20
40
60
80
100
120
Time after injection (min)

Figure 10.

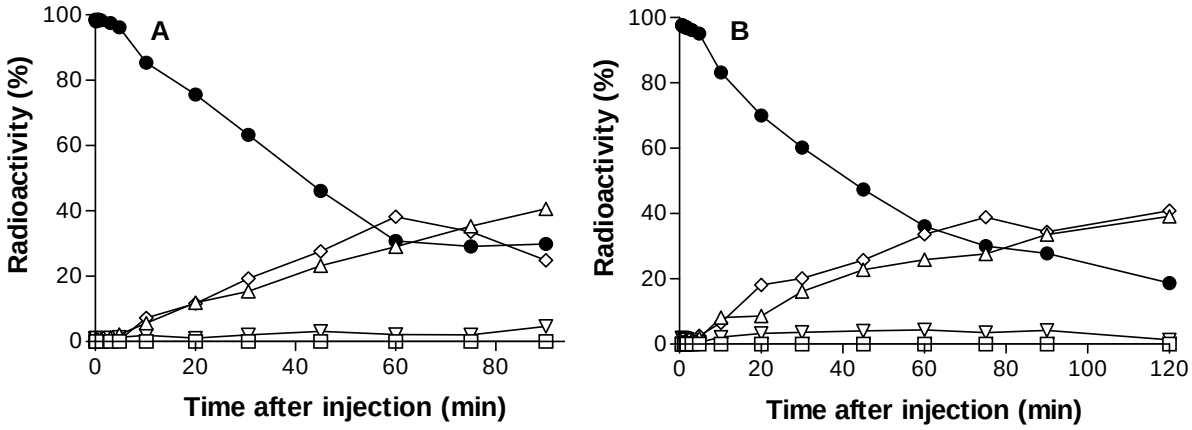
A
B
Radioactivity (%)
Time after injection (min)
0
20
40
60
80
100
120

Figure 11.

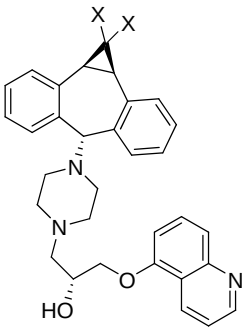

X = Cl, DCPQ
X = F, Zosuquidar